Analysis of the pH- and Ligand-Induced Spectral Transitions of Tryptophanase: Activation of the Coenzyme at the Early Steps of the Catalytic Cycle†

Hiroko Ikushiro,‡ Hideyuki Hayashi,‡ Yasushi Kawata,§ and Hiroyuki Kagamiyama*,‡

Department of Biochemistry, Osaka Medical College, Takatsuki, Osaka 569-8686, Japan and Department of Biotechnology, Faculty of Engineering, Tottori University, Koyama-Minami, Tottori 680-0745, Japan

Received August 12, 1997; Revised Manuscript Received November 3, 1997

ABSTRACT: Tryptophanase has an absorption maximum at 338 nm at high pH and 422 nm at low pH. The 422-nm absorption species has been considered to be the catalytically competent ketoenamine form of the Schiff base of pyridoxal 5′-phosphate with a lysine residue. The 338-nm absorption band showed an intense fluorescence band at 390 nm and not around 500 nm, indicating that the 338-nm absorption species is the substituted aldamine rather than an enolimine form of the Schiff base which has been suggested previously. To explore the mechanism of the enzyme that can exert its catalytic ability at high pH where most of its coenzyme exists as the catalytically incompetent aldamine structure, the reaction of tryptophanase with 3-indolepropionate, a substrate analogue that stops the reaction at the step of the Michaelis complex, was studied at various pH values and analogue concentrations. Kinetic analysis was done based on a scheme involving eight forms of the enzyme, i.e., the liganded and unliganded forms of the ketoenamine, the substituted aldamine structures, and their protonated and deprotonated forms. Kinetic parameters were obtained for each interconversion step. The results showed that the binding of 3-indolepropionate to tryptophanase shifts the equilibrium from the substituted aldamine to the ketoenamine structure over the entire pH region studied. This implies that in the reaction of tryptophanase with tryptophan at high pH, where the enzyme shows maximum activity, the binding of the substrate to the enzyme converts the inactive aldamine form of the coenzyme to the active ketoenamine form. Mechanisms for the activation process, in which a nucleophile is expelled from the aldamine either by steric hindrance of the nucleophile with the ligand or by the negative charge of the ligand α-carboxylate group that stabilizes the aldimine structure, were discussed.

Tryptophanase (L-tryptophan indole-lyase)[1] [EC4.1.99.1] is a microbial pyridoxal 5′-phosphate (PLP[2])-dependent enzyme which catalyzes the hydrolytic cleavage of L-tryptophan to indole, ammonia, and pyruvate. This enzyme also catalyzes the synthesis of tryptophan from indole, pyruvate, and ammonia, as well as α,*β*-elimination, *β*-replacement, and α-hydrogen exchange reactions with various L-amino acids as substrates (*1*, *2*). Tryptophanase is a tetrameric enzyme composed of identical subunits ($M_r \cong 52000$), each containing one molecule of PLP (*3*). In the *E. coli* tryptophanase, PLP forms an internal Schiff base with the side chain of Lys270 (*4*). The overproduction of tryptophanase in *E. coli* cells and the crystallization of the enzyme have been reported (*5*). The X-ray analysis of the *Proteus vulgaris* enzyme is currently in progress (*6*), and a preliminary study of the crystals has been reported for the *E. coli* enzyme (*7*).

The general aspects of the reaction mechanism of tryptophanase have been reviewed (*8*−*10*). Briefly, the catalytic cycle of tryptophanase consists of the following steps: (1) association of the amino acid substrate with the enzyme to form the Michaelis complex; (2) formation of the external aldimine (transaldimination); (3) quinonoid formation by α-proton abstraction from the external aldimine; (4) tautomerization of the indolyl group; (5) elimination of indole and formation of the aminoacrylate Schiff base intermediate; (6) restoration of the internal aldimine (transaldimination); (7) release of aminoacrylate and decomposition to pyruvate and ammonia. This reaction mechanism of tryptophanase has been established by preparation of stable complexes of the enzyme with substrates or their analogues and detailed analysis of their spectroscopic properties (*11*, *12*). Especially, with regard to steps 3 to 7, rigorous studies have been carried out by Phillips and co-workers. Using rapid-scanning stopped-flow spectrophotometry, transient intermediates for these steps have been detected, analyzed, and discussed (*13*−*15*). However, insufficient analyses have been performed for steps 1 and 2. As in the cases of the other PLP-dependent enzymes, the reactions catalyzed by tryptophanase are promoted by the electron-withdrawing ability of the pyridine

† This work was supported by Grants-in-Aid (06680628 to H.H. and 14454160 to H.K.) from the Ministry of Education, Science, Sports, and Culture of Japan, and by a Research Grant (JSPS-RFTF 96L00506) from the Japan Society for the Promotion of Science ("Research for the Future" Program).

* To whom correspondence should be addressed. Tel.: +81-726-83-1221, ext 2645; FAX: +81-726-84-6516, E-mail: med001@art.osaka-med.ac.jp.

‡ Osaka Medical College.

§ Tottori University.

[1] L-Tryptophan indole-lyase [EC 4.1.99.1] is more commonly known by the trivial name of "tryptophanase".

[2] Abbreviations: PLP, pyridoxal 5′-phosphate; SOPC, *S*-(*o*-nitrophenyl)-L-cysteine.

S0006-2960(97)01995-8 CCC: $15.00
Published on Web 02/13/1998

ring of PLP in the PLP−substrate Schiff base (external aldimine). Therefore, the formation of the external aldimine from the Michaelis complex by transaldimination is a prerequisite step of the tryptophanase reaction.

Tryptophanase displays characteristic absorption spectra with maxima at 422 and 338 nm (*3*). The relative intensities of these bands change with pH and with binding of substrates or substrate analogues (*3*, *16*). The absorbance at 422 nm has been attributed to the ketoenamine form of the Schiff base. However, the structure for the absorption at 338 nm has been unclear and several structures, such as a dipolar ionic form of aldimine, a substituted aldamine, and an enolimine tautomer have been proposed (*3*, *11*, *17*). It is well-known that tryptophanase is catalytically more competent at alkaline pH, where the 338-nm absorbing form is the major species (*3*). However, the stopped-flow studies on the quinonoid formation with the inhibitor, L-ethionine, showed that the 422-nm species is the active form that reacts with the substrate (*11*). This indicates that tryptophanase must change its coenzyme structure to the active form to metabolize a substrate. Therefore, it is interesting to know how tryptophanase converts its coenzyme structure from the 338-nm absorbing form to the 422-nm absorbing form in the early step of the reaction cycle. To analyze the molecular mechanism, we first studied the structure of the 338-nm species using fluorescent spectroscopy. Next, we analyzed the binding of 3-indolepropionate, a substrate analogue, which mimics the Michaelis complex of tryptophanase with tryptophan. The equilibrium and the transition process of the binding of the substrate analogue to the enzyme were studied using static and stopped-flow spectroscopic measurements. In this work, we examine the structure of the coenzyme and its involvement in catalysis using four kinds of enzyme species in their liganded and unliganded forms, with relation to the early steps of the reaction sequence catalyzed by tryptophanase.

MATERIALS AND METHODS

Chemicals. L-Tryptophan and 3-indolepropionate were obtained from Nacalai Tesque (Kyoto, Japan). 3-Indolepropionic acid was recrystallized from chloroform before use. *S*-(*o*-Nitrophenyl)-L-cysteine (SOPC[2]) for enzyme assays was synthesized from L-cysteine and 2-fluoronitrobenzene as previously described (*18*). All other chemicals were of the best commercially available grade.

Expression of the Enzyme. The *Bam*HI−*Hin*dIII fragment of the plasmid pMD6B (*5*) containing the *tnaA* gene was ligated to the *Bam*HI−*Hin*dIII site of pUC118. The resultant plasmid, named pUC118-*tnaA*, was used to transform *E. coli* MD55 which lacks tryptophanase. The transformed *E. coli* cells were grown in media containing 0.5% yeast extract (Oriental Yeast, Tokyo, Japan), 1.0% Polypepton (Nihon Pharmaceutical, Tokyo, Japan), and 1.0% NaCl for 24 h, and the cells were harvested in the stationary phase. From a 1-L culture, 3.0 g of the bacterial cells were collected. The MD55/pUC118-*tnaA* cells expressed about 30 times more tryptophanase than JM109 cells that had been cultured similarly.

Assay of the Enzyme Activity. Routine activity assays were performed with SOPC in 100 mM potassium phosphate buffer (pH 8.0) at 25 °C, by following the absorbance decrease at 370 nm ($\Delta\epsilon = -1860$ M^{-1} cm^{-1}) (*19*).

Purification of the Enzyme. The purification of tryptophanase was performed as follows. All preparation procedures were performed at 4 °C. All buffers used in the purification procedures contained 0.1 mM EDTA, 5 mM 2-mercaptoethanol, and 20 μM pyridoxal phosphate. The cells (3.0 g wet weight) were suspended in 100 mL of 100 mM potassium phosphate buffer (pH 7.5) and disrupted sonically (Branson Sonic Power Co., Sonifier model 350, 20 kHz) for 9 min. The intact cells and debris were removed by centrifugation (10000*g*, 30 min). After the addition of ammonium sulfate (final concentration, 30% saturation) and centrifugation (10000*g*, 60 min), the supernatant solution was applied to a Phenyl Sepharose CL-4B column (2.5 × 20 cm) equilibrated with 20 mM potassium phosphate buffer (pH 7.5) containing 30% ammonium sulfate. The proteins were eluted with 1 L of linearly decreasing ammonium sulfate (30 to 0%) and potassium phosphate (20 to 1 mM) concentrations. The pooled active fractions were applied to a DEAE-Toyopearl 650M column (2.5 × 20 cm) equilibrated with 5 mM potassium phosphate buffer (pH 7.5). The enzymes were eluted with a 1-L linear gradient from 0 to 200 mM KCl in 5 mM potassium phosphate buffer (pH 7.5). The active fractions were collected and applied to a hydroxyapatite column (2.5 × 20 cm) equilibrated with 10 mM potassium phosphate buffer (pH 7.5). The enzyme was eluted with a 1-L linear gradient formed with 10 and 100 mM potassium phosphate buffer (pH 7.5).

Spectrophotometric Measurements. Absorption and fluorescence spectra of tryptophanase were recorded with a Hitachi spectrophotometer U-3300 and a Hitachi spectrofluorometer Model 850, respectively, at 25 °C. The buffer solution for the absorption measurements contained 100 mM potassium phosphate and 0.1 mM EDTA. Tryptophanase was equilibrated with the above buffer by gel filtration using a PD-10 (Sephadex G-25) column (Pharmacia Biotech, Uppsala, Sweden) prior to the measurement. Protein concentrations were generally 1−2 mg/mL. Spectrophotometric titrations of tryptophanase with 3-indolepropionate were performed under the same conditions used for the measurements of the absorption spectra. The pH was measured before and after each spectroscopic measurement.

Stopped-flow spectrophotometry was performed using the Applied Photophysics (Leatherhead, UK) SX.17MV system. The dead time for this system was generally 2.0 ms under a pressure of 500 kPa. The reaction of tryptophanase with 3-indolepropionate was analyzed by monitoring the absorption change at 338 or 422 nm. The exponential absorption changes were analyzed with the program provided with the SX.17MV stopped-flow spectrophotometer. The apparent rate constants obtained were then analyzed for their dependency on the substrate concentration, and kinetic parameters were obtained by nonlinear regression with the software Igor Pro (ver. 2.04, WaveMetrics, Lake Oswego, OR).

pH-Jump Experiments. To measure the rates over a broad range of the final pH values, several initial pHs were used. For measurements at low final pH, the initial pH of a buffered enzyme solution was adjusted to pH 9.0. The initial pH was 7.0 for a high final pH. Tryptophanase (20 mg/mL) was equilibrated with a 100 mM potassium phosphate buffer containing 1 mM EDTA by gel filtration using a PD-10 column. The enzyme was diluted with the same buffer to a concentration of 4.0 mg/mL prior to the experiment. This

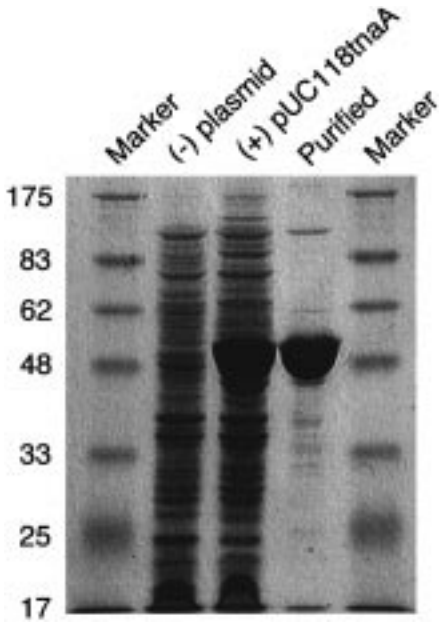

FIGURE 1: SDS-polyacrylamide gel electrophoresis of crude extracts and purified tryptophanase. Samples were treated with 2% SDS in 63 mM Tris-HCl buffer (pH 6.8) containing 5% 2-mercaptoethanol, 10% glycerol, and 0.01% bromophenol blue at 90 °C for 3 min. The prepared samples (5 μL) were analyzed by SDS-polyacrylamide gel electrophoresis on a 10% gel and stained with Coomassie blue. Prestained Protein Marker, Broad Range, from New England Biolabs was used as the molecular mass standard.

solution was pushed against 100 mM potassium phosphate buffer containing 1 mM EDTA to give final pH values of 6.59, 6.77, 6.89, 7.02, 7.19, 7.49, 7.85, 8.15, 8.30, 8.57, and 8.64.

Other Methods. pH values were determined with a Horiba Model F-23 digital pH/Ion meter (Horiba, Kyoto, Japan) at 25 °C. Protein concentration was determined with a BCA protein assay kit (Pierce Chemical, Rockford, IL) using bovine serum albumin as a standard. SDS-electrophoresis was carried out with an SDS-Tris system using 10.0% polyacrylamide gel according to the procedure described by Laemmli (*20*).

RESULTS

Overproduction and Purification of Tryptophanase. The overproduction of tryptophanase has been already reported (*5*). To improve the expression level, we constructed a high-copy plasmid harboring the *tnaA* gene by ligating the *Bam*HI−*Hin*dIII fragment of pMD6B (*5*) to the *Bam*HI−*Hin*dIII site of pUC118. The resultant plasmid was used to transform the *E. coli* MD55 cells. The MD55/pUC118-*tnaA* cells expressed about twice as much tryptophanase as the MD55/pMD6B cells when they were cultured similarly. The holo form of tryptophanase was purified using three kinds of chromatography without the heat treatment or the ammonium sulfate precipitation. About 300 mg of protein could be obtained from 3 g of cells used as a starting material in 70% yield. As shown in Figure 1, the expressed tryptophanase was the major component of the bacterial proteins. The purified tryptophanase was homogeneous as judged by the criteria of SDS-polyacrylamide gel electrophoresis. Table 1 summarizes the purification of the enzyme. It could be stored at 4 °C in sterile capped vials for up to 1 month in a

Table 1: Purification of Tryptophanase from *E. coli* MD55/pUC118−*tnaA*

steps	total activity[a] (μmol/min)	total protein (mg)	specific activity (μmol/min/mg)	yield (%)
crude extract	17100	903	18.9	100
phenyl sepharose CL−4B	13200	507	26.0	77
DEAE-toyopearl 650M	12500	328	38.1	73
hydroxyapatite	11600	276	42.0	68

[a] Activity is expressed as μmol of SOPC cleaved per min at 25 °C in 100 mM potassium phosphate buffer, pH 8.0.

Scheme 1: Structures of the Ketoenamine Form (**a**), the Enolimine Form (**b**), and the Substituted Aldamine Form (**c**)

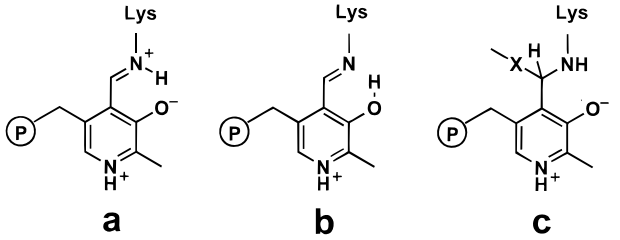

100 mM potassium phosphate buffer (pH 7.5) containing 0.1 mM EDTA and 20 μM PLP without evident deterioration.

Absorption and Fluorescence Spectra of Tryptophanase. The absorption spectra of tryptophanase in the pH range between 6.5 and 9.5 are shown in Figure 2A. Tryptophanase showed absorption maxima at 422 nm in the acidic pH region and at 338 nm in the alkaline pH region without a clear isosbestic point. This observation was already reported by several groups using various buffer systems (*3*, *11*, *13*, *17*, *21*). Our observation using potassium phosphate buffer confirmed those results. Figure 2B shows the plot of the apparent molar extinction coefficient of each spectral band as a function of pH. The apparent pK_a value of the coenzyme chromophore (pK_a^E) was found to be 7.60. Tryptophanase emitted fluorescence at 385 and 512 nm upon excitation at 338 and 422 nm, respectively (Figure 3). When the fluorescence was monitored at 385 and 512 nm, the excitation spectra exhibited maxima at 338 and 422 nm, respectively, corresponding to the absorption maxima of tryptophanase. Fluorescence intensity was much higher at 385 nm than at 512 nm in the alkaline pH region, although the peak height at 512 nm increased and that at 385 nm decreased with decreasing pH. Isom and DeMoss (*22*) also observed a similar pH effect on the fluorescence emission spectra of tryptophanase from *Bacillus alvei*. It is known that a substituted aldamine (Scheme 1c) gives a maximum emission wavelength at around 390 nm when excited at around 330 nm, whereas the enolimine structure (Scheme 1b) emits fluorescence with a maximum intensity at around 510 nm (*23*, *24*). When tryptophanase was treated with phenylhydrazine, the absorption bands at both 338 and 422 nm were lost, and the resultant apo-tryptophanase lacked the fluorescence bands at 385 and 515 nm (data not shown).

pH-Jump Study of Tryptophanase. As tryptophanase shows protonated and deprotonated structures involving the coenzyme, the catalytic mechanism of the enzyme is considered to be closely related to the protonation/deprotonation events. Therefore, we analyzed the pH-induced

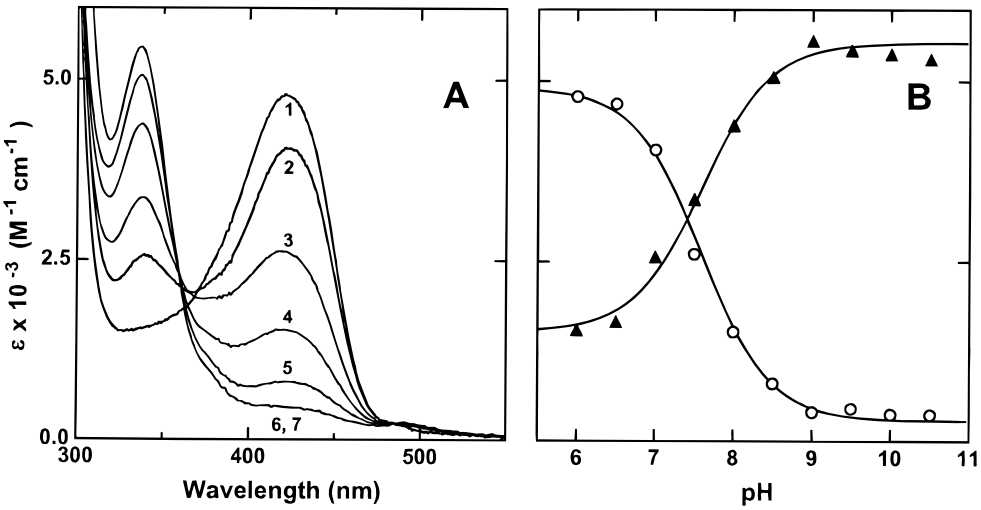

FIGURE 2: pH-dependent absorption changes of tryptophanase at 25 °C. (A) Absorption spectra at pH 6.5 (curve 1), 7.0 (2), 7.5 (3), 8.0 (4), 8.5 (5), 9.0 (6), and 9.5 (7). Curves 6 and 7 are almost superimposable. (B) Titration curves of the apparent molar extinction coefficients at 422 nm (○) and 338 nm (▲) for tryptophanase. The solid line represents the theoretical curve using eq 8. The spectra were taken in 100 mM potassium phosphate buffer containing 0.1 mM EDTA at a protein concentration of 1 mg/mL in a 1-cm cell.

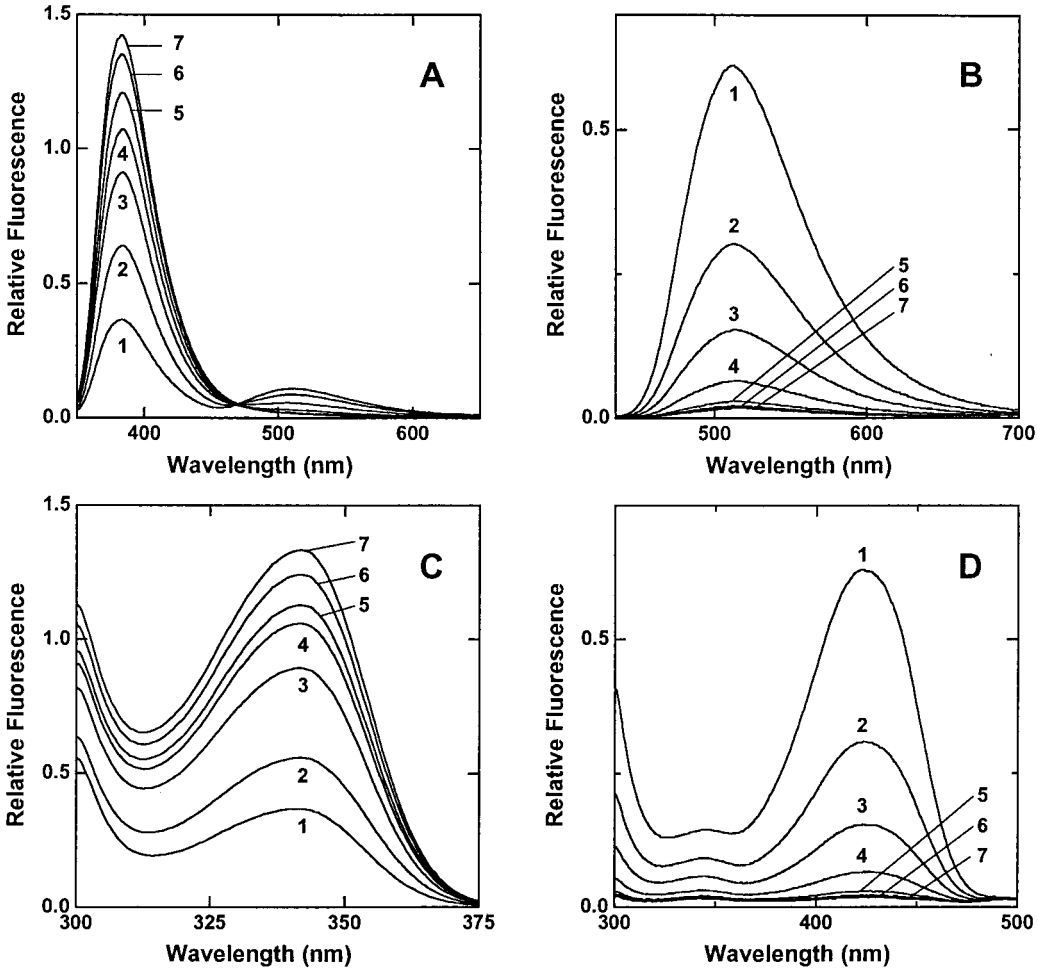

FIGURE 3: Fluorescence spectra of tryptophanase at 25 °C. (A) Fluorescence emission spectra at pH 6.5 (curve 1), 7.0 (2), 7.5 (3), 8.0 (4), 8.5 (5), 9.0 (6), and 9.5 (7) upon excitation at 338 nm. (B) Fluorescence emission spectra at pH 6.5 (curve 1), 7.0 (2), 7.5 (3), 8.0 (4), 8.5 (5), 9.0 (6), 9.5 (7) upon excitation at 422 nm. (C) Fluorescence excitation spectra at pH 6.5 (curve 1), 7.0 (2), 7.5 (3), 8.0 (4), 8.5 (5), 9.0 (6), and 9.5 (7) with emission wavelength of 385 nm. (D) Fluorescence excitation spectra at pH 6.5 (curve 1), 7.0 (2), 7.5 (3), 8.0 (4), 8.5 (5), 9.0 (6), and 9.5 (7) with emission wavelength of 512 nm. The spectra were taken by the method described in the legend of Figure 2.

spectral change of tryptophanase by the pH-jump method. When the pH of a solution containing tryptophanase was rapidly changed from 9.2 to low pH values, an increase in the absorbance at 422 nm and a concomitant decrease in the absorbance at 338 nm were observed over a period of several seconds. When the pH of an enzyme solution was rapidly increased from low values, an increase in the 338-nm absorption and a concomitant decrease in the 422-nm

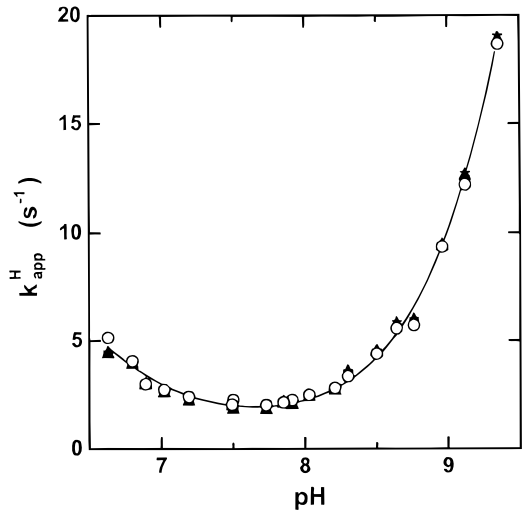

FIGURE 4: The apparent rate constant (k_{app}^{H}) for the spectral change at 422 (○) and 338 nm (▲) in the pH-jump experiments plotted as a function of the final pH. Data are means for the three separate determinations, and vertical bars denote SDs. The solid line represents the theoretical curve obtained using eq 10 as described in Appendix with the rate constant values of $k_1 = 76.7\ s^{-1}$, $k_2 = 0.397\ s^{-1}$, $k_5 = 0.605\ s^{-1}$, and $k_6 = 12.4\ s^{-1}$. These values were obtained by nonlinear regression (see Appendix).

Scheme 2: Structures of the Coenzyme in Tryptophanase

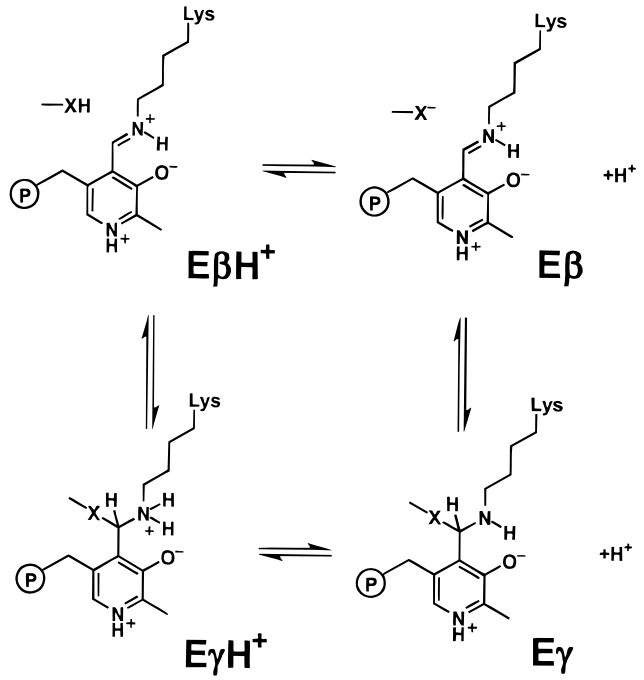

absorption were observed. Under most conditions these changes followed first-order kinetics. The apparent rate constant (k_{app}^{H}) calculated from the absorbance change at 422 nm was equal to that at 338 nm. The value of k_{app}^{H} was dependent only on the final pH but independent of the initial pH and the enzyme concentration. The k_{app}^{H} value was plotted against the final pH value (Figure 4). The result can be rationalized as shown in Scheme 2, in which the interconversion of the absorption bands at 422 and 338 nm reflects the structural change of the internal Schiff base; ketoenamine form (β form[3]) and substituted aldamine form (γ form), and the protonation−deprotonation equilibrium of each form of the enzyme is assumed (E_β, $E_\beta H^+$, E_γ, and $E_\gamma H^+$ in Scheme 3). The solid line shown in Figure 4 was drawn theoretically using eq 10 described in Appendix. The pK_a values of each enzyme form were obtained as p$K_a^\beta = 9.87$ and p$K_a^\gamma = 6.27$. The rate constants for interconversion between E_β and E_γ, and that between $E_\beta H^+$ and $E_\gamma H^+$, were also obtained. These kinetic parameters are summarized in Scheme 3.

Scheme 3: Interconversion between the Enzyme Species with Different Protonation, Liganded, and Coenzyme Structures[a]

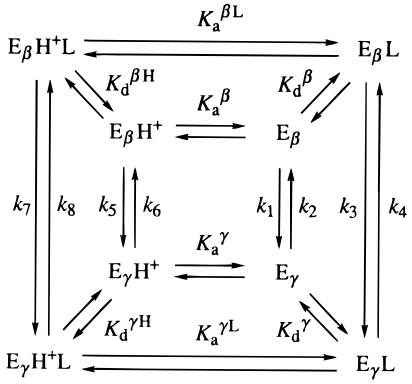

pK_a^β = 9.87	$k_1 = 76.7\ s^{-1}$
pK_a^γ = 6.27	$k_2 = 0.397\ s^{-1}$
p$K_a^{\beta L}$ = 9.53	$k_3 = 0.365\ s^{-1}$
p$K_a^{\gamma L}$ = 8.40	$k_4 = 3.01\ s^{-1}$
K_d^β = 0.0920 mM	$k_5 = 0.605\ s^{-1}$
K_d^γ = 146 mM	$k_6 = 12.4\ s^{-1}$
$K_d^{\beta H}$ = 0.201 mM	$k_7 = 0.422\ s^{-1}$
$K_d^{\gamma H}$ = 1.08 mM	$k_8 = 46.3\ s^{-1}$

[a] E, H^+ and L represent tryptophanase, proton and 3-indolepropionate, respectively. β and γ mean that the PLP-Lys Schiff base of tryptophanase is in a ketoenamine (Scheme 1a; β form) and in a substituted aldamine form (Scheme 1c; γ form), respectively. K_a^x and K_a^{xL} are the acid dissociation constant for the free and the 3-indolepropionate bound x-form of the enzyme (E_x and E_xH), respectively. K_d^x and K_d^{xH} are the dissociation constant for 3-indolepropionate of the unprotonated and the protonated x-form of the enzyme, respectively.

Binding of 3-Indolepropionate at Various pHs. 3-Indolepropionate binds noncovalently to the active site of tryptophanase, because it has no amino group to form an external Schiff base with PLP in the active site (*16*, *25*). So the complexes of tryptophanase with 3-indolepropionate are considered to mimic the Michaelis complexes of tryptophanase with the substrate and the binding of 3-indolepropionate to tryptophanase appears to be a good model for investigation of structural changes in the enzyme upon formation of the Michaelis complex. The addition of 3-indolepropionate to tryptophanase gave rise to an intense absorption band at 422 nm and a less intense band at 338 nm (Figure 5A), indicating that the aldamine form of the PLP-Lys Schiff base (γ form)

[3] With regard to the naming of the species of tryptophanase, we followed that used by June et al. (*11*) in which the α form was the inactive holoenzyme predominant in the absence of monovalent cations, the β form was the 422-nm absorbing species, and the γ form was the 338-nm absorbing species. The present study is conducted in a 100 mM potassium phosphate buffer system; therefore, the enzyme is considered to be either in β or in γ form (*3*).

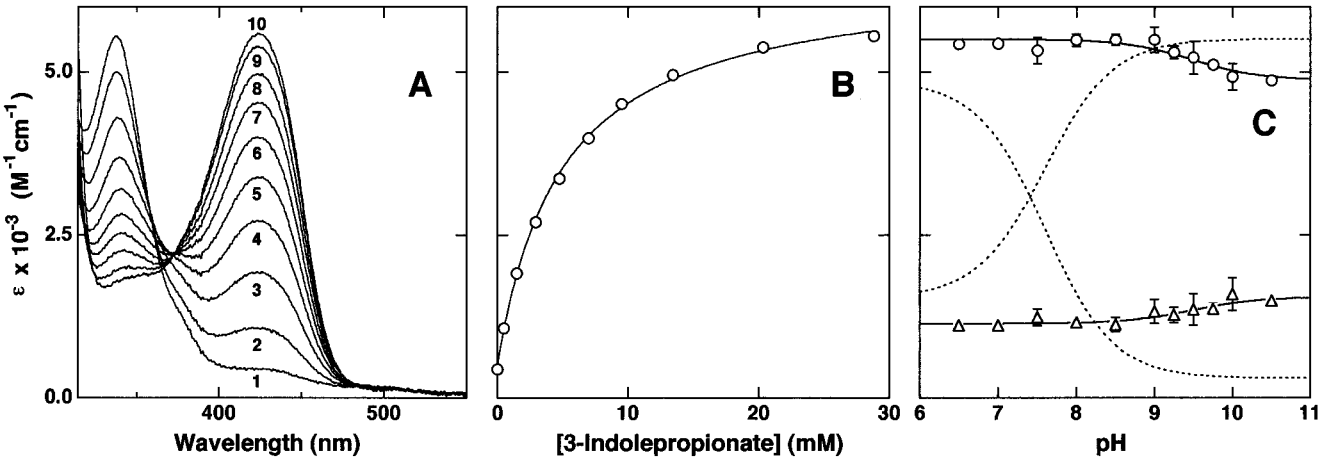

FIGURE 5: Binding of 3-indolepropionate to tryptophanase. (A) Absorption spectra of tryptophanase in the absence (curve 1) and presence of 0.50 (2), 1.48 (3), 2.91 (4), 4.76 (5), 6.98 (6), 9.50 (7), 13.4 (8), 20.3 (9), and 28.8 mM (10) 3-indolepropionate at pH 9.25 at 25 °C. (B) Plot of the apparent molar extinction coefficients at 422 nm for tryptophanase against the concentration of 3-indolepropionate. The solid line represents the best-fit curve with an apparent dissociation constant of K_d^{app} = 5.05 mM. (C) The apparent molar extinction coefficients at 422 nm (○) and 338 nm (△) in the presence of a saturating amount of 3-indolepropionate were extrapolated and plotted against pH. The data were fit to the theoretical curves with pK_a^{EL} = 9.48. The dotted lines are the titration curves in the absence of 3-indolepropionate shown in Figure 2B. The experiments were performed in the buffer solutions as described in the legend of Figure 2.

changed to the ketoenamine form (β form). These observed spectral changes showed a hyperbolic dependency on the analogue concentration (Figure 5B), and from this plot the apparent dissociation constant, K_d^{app}, for 3-indolepropionate was determined by monitoring the spectral changes. The apparent molar extinction coefficients of the two spectral bands in the fully 3-indolepropionate-bound enzyme were obtained by extrapolation to a saturating amount of 3-indolepropionate and were plotted against the pH (Figure 5C). The apparent pK_a value of the analogue-bound enzyme (pK_a^{EL}) was found to be 9.48, showing that the apparent pK_a of tryptophanase increased from 7.60 to 9.48 upon binding of 3-indolepropionate. The shift in the enzyme pK_a upon binding of ligands and the pH dependency of the ligand's K_d^{app} values are closely related events, which can be analyzed by assuming a thermodynamic cycle shown in Scheme 3. The log(K_d^{app}) value is dependent on pH, as expressed by eq 14 described in Appendix. The plots of log(K_d^{app}) against pH are shown in Figure 6, and the theoretical curves fitted well to the experimental data.

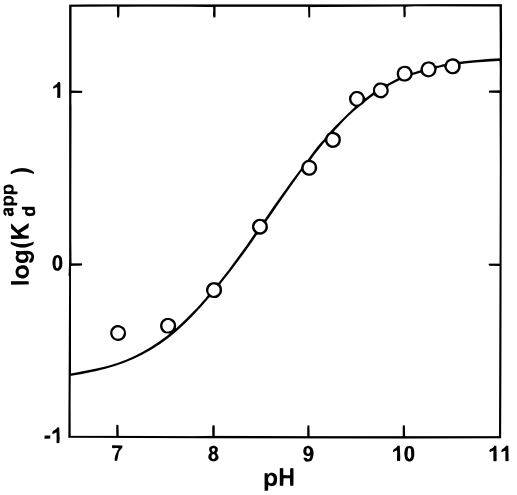

FIGURE 6: Effect of pH on log(K_d^{app}) of tryptophanase for 3-indolepropionate. K_d^{app} is expressed in mM. The solid line represents the theoretical curve drawn according to eq 14. The experiments were performed in the buffer solutions as described in the legend of Figure 2.

The time-dependent changes in the absorbance at 422 and 338 nm of tryptophanase on reaction with 3-indolepropionate at various pHs were studied in a stopped-flow spectrophotometer. Upon mixing the enzyme with various concentrations of 3-indolepropionate, a rapid increase in the absorbance at 422 nm and a concomitant rapid decrease at 338 nm were observed. These absorbance changes proceeded exponentially, and the apparent rate constants (k_{app}^{L}) were obtained from these reaction curves. The values of k_{app}^{L} were varied with the concentration of the ligand and with the pH value and showed a nonlinear relationship with ligand concentration as shown in Figure 7. The experimental data were fitted well to the theoretical curves drawn according to eq 18 where k_3, k_4, k_7, and k_8 are adjustable parameters. Using eqs 2−5, 15, and 16, K_d values and the rate constants were obtained and are summarized in Scheme 3. The values of k_{app}^{L} at higher pH were much smaller than those at lower pH, and the saturation was not detected in the range of the tested analogue concentration. This is because of the high K_d^{γ} value (146 mM) compared to the $K_d^{\gamma H}$ (1.08 mM), and the small k_4 value (3.01 s^{-1}) compared to k_8 (46.3 s^{-1}).

DISCUSSION

Tryptophanase shows absorption maxima at 338 and 422 nm. Morino and Snell (*3*) ascribed the 338-nm species to a dipolar ionic form of the internal PLP-lysine aldimine or to a substituted aldamine in which a second ligand has been added across the double bond of the aldimine. On the basis of the inactivation of enzyme by borohydride reduction, they concluded the structure of the 338-nm species of tryptophanase to be a dipolar ionic form of the aldimine. However, the dipolar ionic form absorbs at about 360 nm in aspartate aminotransferase and in the model systems containing Schiff bases of *N*-methylated PLP (*26*). In some PLP-dependent enzymes, the nature of the 338-nm-absorbing species has been suggested to be either the enolimine tautomer of the

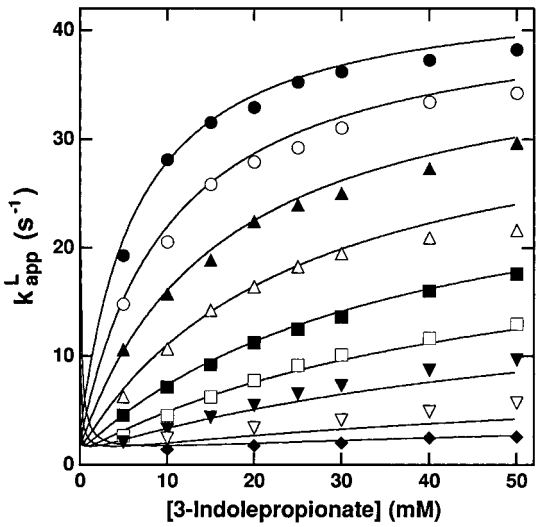

FIGURE 7: Effects of the concentration of 3-indolepropionate on the rate of binding of 3-indolepropionate to tryptophanase. The apparent rate constants (k_{app}^{L}) for the spectral change at 422 nm in the stopped-flow experiments were plotted as a function of 3-indolepropionate concentration. Data are means of five separate determinations, and vertical bars denote SDs. Each solid line represents the theoretical curve constructed according to Scheme 3 (see Appendix for details). The experiments were performed in the buffer solutions as described in the legend under Figure 2 at pH 7.00 (●), 7.25 (○), 7.50 (▲), 7.75 (△), 8.00 (■), 8.25 (□), 8.50 (▼), 9.00 (▽), and 9.50 (◆).

protonated PLP-lysine aldimine (*23*, *27*, *28*) or the substituted aldamine (*24*, *29*, *30*). In the case of tryptophanase, it has been unclear as to which structure, the enolimine tautomer or the substituted aldamine, can account for the 338-nm absorption. These two species can be distinguished by fluorescence spectroscopy (*27*, *28*, *31*). The enolimine tautomer should show fluorescence at around 500 nm but not at around 390 nm upon excitation at around 330 nm. Because there are no double bonds conjugated with the pyridine ring, the substituted aldamines and other phosphopyridoxyl derivatives show fluorescence at around 390 nm with excitation at 330 nm. The fluorescence spectra of tryptophanase showed an emission band at 385 nm with excitation at 338 nm (Figure 3). All these observations agree with the conclusion that the 338-nm absorption of tryptophanase should be attributed to the substituted aldamine structure. The structure of the adduct will be discussed below.

In acid−base titration experiments (Figure 2), the obtained value of apparent pK_a^E was 7.60. Morino and Snell (*3*) originally reported the acid−base titration of tryptophanase in imidazole and carbonate buffers as a simple curve with a single pK_a value of 7.2. A single pK_a value of either 7.4 (*21*) or 7.5 (*13*) also has been reported using potassium phosphate buffer. Some difference in the pK_a values may be due to the variation in the buffer system.[4] June et al. (*11*) obtained a value of 8.1 from the spectral changes on pH-jump using the buffers TES and Bicine. Metzler et al. (*17*) reported that the titration of tryptophanase in potassium phosphate buffer was described most simply as resulting from two consecutive proton dissociations with pK_a values of about 7.36 and 7.76. The latter two groups proposed the ketoenamine and the enolimine structures to be responsible for the absorption species at 422 and 338 nm, respectively, and that each species has a conformational manifold differing only in the state of protonation at the pyridinium nitrogen. In both aspartate aminotransferase and tyrosine phenol-lyase, an active site aspartate residue (Asp222 and Asp214, respectively) is located near the pyridinium nitrogen of PLP and is thought to increase the pK_a value of the nitrogen (*32*−*34*). The corresponding conserved residue, Asp227, of tryptophanase is thought to be located at this site and also to stabilize the protonated pyridinium nitrogen of PLP. It is therefore difficult to consider the deprotonation at this part of PLP. Based on the observation that the 338-nm absorption species is most probably the substituted aldamine (see above), we propose another model shown in Scheme 2. The scheme involves two enzyme species β and γ. β is the ketoenamine form and γ is the substituted-aldamine form.[5] Both $E_\beta H^+$ and E_β show an absorption maximum at 422 nm, while $E_\gamma H^+$ and E_γ absorb at 338 nm. A group (XH) was considered to form an adduct with the imino group of the Schiff base. The k_5/k_6 value of 0.05 indicates that the equilibrium between $E_\beta H^+$ and $E_\gamma H^+$ shifts to $E_\beta H^+$, and the k_1/k_2 value of 192 indicates that the equilibrium between E_β and E_γ shifts to the E_γ. As a result, $E_\beta H^+$ and E_γ are the dominant species in the acidic and the alkaline region, respectively. This equilibrium shift can be reasonably explained by the structures shown in Scheme 2, since the deprotonated form of the group (X^-) is considered to be more favorable for forming the adduct. The substituted aldamine (γ) form of tryptophanase is enzymatically inactive because of the sp^3 hybridization structure at C-4′ of PLP.

Scheme 2 differs from the scheme presented by June et al. (*11*) only in that protonation/deprotonation occurs at a group beside the coenzyme rather than the pyridine nitrogen of the coenzyme and that the 338-nm absorbing structure is the substituted aldamine rather than the enolimine structure. Therefore, it appears that the kinetic results presented in this paper may also be explained by the scheme of June et al. (*11*). There is no remarkable difference between pK_a^β and $pK_a^{\beta L}$, whereas there is a large difference between pK_a^γ and $pK_a^{\gamma L}$ by about 2.0 units. If we take the scheme of June et al. (*11*), the binding of indolepropionate increases the pK_a of the pyridine nitrogen of the enolimine structure without altering that of the ketoenamine structure. It is, however, difficult to explain how the carboxylate group of indolepropionate has an electrostatic effect on the enolimine structure and not on the ketoenamine structure. We, therefore, tried to discuss based in Scheme 2 the effect of the ligand binding on the shift in equilibrium between the four species.

[4] The absorption band at 422 nm nearly completely disappears at alkaline pH in a potassium phosphate buffer system, while significant absorption at 422 nm remains at alkaline pH in other buffer systems, such as Good's buffers, carbonate, and pyrophosphate. This residual absorption may be partly ascribed to the binding of the buffer anions to the active site which electrostatically increase the fraction of the protonated aldimine forms (Scheme 2), although the reason for the fact that phosphate ion is inert is not known at present.

[5] Although the presence of the dipolar ionic form of aldimine with maximum absorption at around 360 nm has been reported (*11*, *17*), we ignored the 360-nm absorbing species in this analysis because of its minor population. The presence of the 360-nm species may be one reason for the lack of a clear isosbestic point in the acid−base titration of tryptophanase.

As the three-dimensional structure of the active site of *E. coli* tryptophanase has not been fully elucidated except for the monovalent-cation-binding site (*35*), we have no structural information about the structure of XH that is supposed to form an adduct with the PLP-Lys270 aldimine. On the other hand, detailed crystallographic structures have been reported for the *Citrobacter freundii* tyrosine phenol-lyase (*34*). Considering the close similarity of the primary structures of the two enzymes, with almost complete conservation of the active site residues of the *C. freundii* tyrosine phenol-lyase in the *E. coli* tryptophanase, we can anticipate that the structural data of *C. freundii* tyrosine phenol-lyase can be used for the discussion of the active site structure of tryptophanase. The structure around the PLP-Lys257 aldimine of tyrosine phenol-lyase shows that Lys256, corresponding to Lys269 of tryptophanase, interacts with the monovalent cation via a water molecule. The size of the monovalent cation affects the conformation of the PLP-Lys257 aldimine and hence the activity of tyrosine phenol-lyase, through the side chain of Lys256 and the 256−257 main chain (*35*). Tryptophanase and tyrosine phenol-lyase are activated by monovalent cations, such as K^+ and NH_4^+, in a similar way. This strongly suggests that the corresponding residue, Lys269, of tryptophanase has a similar role of connecting the cation binding site and the PLP-Lys270 aldimine. This indicates that the side chain of Lys269 interacting with the cation-binding site cannot form an adduct with the PLP-Lys270 aldimine. That XH is less likely the amino group of Lys269 is further supported by a brief chemical consideration as follows. If we consider X^- to be a free amino group and XH an ammonium group, there is no direct interconversion between $E_\beta H^+$ and $E_\gamma H^+$, because an ammonium group cannot attack an imine bond nor can it be formed directly from a substituted aldamine. As a result, k_5 and k_6 are zero, and we cannot fit the experimental result of Figure 4 to eq 10.

Careful investigation of the active site structure of tyrosine phenol-lyase shows that there are no other residues, the side chain of which can interact with the PLP aldimine. 3-(4-Hydroxyphenyl)propionate, which is a substrate analogue corresponding to 3-indolepropionate in this study, binds to only one subunit of the dimer in the crystal (*34*). Comparison of the two subunits showed that in the unliganded subunit a hydrogen-bonding network is formed from the guanidinium group of Arg404, the substrate-carboxylate-binding residue, to the hydroxy group of Tyr71 via three water molecules, Wat154, Wat194, and Wa195. These water molecules exist at the *re* face of the aldimine, and Wat195 is 4.42 Å from C4′ of PLP. In the liganded subunit, these water molecules are replaced by 3-(4-hydroxyphenyl)propionate. Therefore, we can consider that, in tryptophanase, a water molecule which may locate at the *re* face of the aldimine is XH. The hydroxy group of the adduct formed between the aldimine and the water molecule would interact unfavorably with the substrate analogue 3-indolepropionate. When 3-indolepropionate binds to either $E_\beta H^+$ or E_β, the released water molecule or the hydroxide ion can be easily expelled by the ligand. This can explain the equilibrium shift from $E_\gamma H^+L$ ($E_\gamma L$) to $E_\beta H^+L$ ($E_\beta L$), as indicated by the kinetic data $k_3/k_4 = 0.12$ and $k_7/k_8 = 0.01$, and the higher value of K_d^γ compared with those of K_d^β and $K_d^{\beta H}$. Compensation of the positive charge of the protonated nitrogen of the aldamine ($E_\gamma H^+$) by the carboxylate group of 3-indolepropionate can be considered to increase the pK_a value of the aldamine ($pK_a^{\gamma L} = 8.40$ versus $pK_a^\gamma = 6.27$). The binding of indolepropionate displaces the water molecule in $E_\beta H^+$ and the hydroxide ion in E_β, both of which are considered to remain in the vicinity of the active site but are away from indolepropionate.[6] Therefore, the electrostatic effect of indolepropionate on the water molecule (XH) is not so large as to change its pK_a value ($pK_a^{\beta L} = 9.53$ versus $pK_a^\beta = 9.87$). The removal of the nucleophilic group from the adduct on the ligand binding can be also explained by electrostatic interaction of the coenzyme with the ligand. Because the negative charge of 3-indolepropionate stabilizes the positive charge at the coenzyme, $E_\beta H^+L$, $E_\beta L$, and $E_\gamma H^+L$ become dominant by the binding of the analog to the enzyme. As a result, the values of $K_d^{\beta H}$, K_d^β, and $K_d^{\gamma H}$ are quite small compared with that of K_d^γ. The complicated configuration around C-4′ of PLP of $E_\gamma H^+$ may be the reason for the relatively high value of $K_d^{\gamma H}$ compared with K_d^β and $K_d^{\beta H}$.

Another possibility to be considered for the reason behind the shift in equilibrium between the four enzyme forms on ligand binding is the ligand-induced conformational change of the enzyme protein. The 3-(4-hydroxyphenyl)propionate-liganded and unliganded subunits of tyrosine phenol-lyase (*34*; PDB entry code 2TPL) can be almost completely superimposed, with a root-mean-square deviation of the backbone atoms of only 0.16 Å. Although the possibility that this results from the crystal packing force cannot be ruled out, this suggests that tyrosine phenol-lyase and its closely related enzyme tryptophanase undergo little domain movement on binding of ligands. We therefore consider that the interaction between the ligand and the aldamine, most probably the adduct formed between the aldimine and a water molecule, is the main driving force that converts the aldamine structure of the coenzyme (γ form) to the ketoenamine structure (β form).

Our results well account for the fact that tryptophanase can be catalytically active in alkaline pH even though the inactive form of the free enzyme is the major species in this pH region. That is, the binding of the substrate to the enzyme, like indolepropionate, converts the γ form to the β form. The resultant E_β (or $E_\beta H^+$) can undergo transaldimination with the substrate amino group to form the external aldimine, which is the prerequisite structure for subsequent catalysis. The nature of XH is still speculative, and it is important to identify the group. To verify the PLP structure proposed by us and to fully understand the reaction mechanism of tryptophanase, the information about the three-dimensional structure of this enzyme, especially at high pH, is required. The crystallization and X-ray diffraction studies of the holotryptophanase from *E. coli* are in progress.

[6] If the water molecule and the hydroxide ion are removed from the active site, $E_\beta H^+L$ and $E_\beta L$ should be treated as a single species ($E_\beta H^+L$). In such a case, the equations that describe the ligand binding are derived from eq 18 by $1/K_d^\beta \rightarrow 0$, $k_3/K_d^\beta \rightarrow (k_3°/K_d^{\beta H})([H^+]/K_a^\beta)$, and $k_4 \rightarrow k_4°[H^+]$, where $k_3°$ and $k_4°$ are the rate constants for the interconversion between $E_\beta H^+L$ and $E_\gamma L$. However, the data of Figure 7 did not fit well to eq 18 obtained in this way. From this, we consider that the water molecule and the hydroxide ion still remain in the active site.

APPENDIX

Analysis of the Interconversion among the Different Ionic and Liganded Species of the β and γ Form of Tryptophanase. According to Scheme 3, K_a^{γ}, K_d^{γ}, $K_d^{\gamma H}$, $K_a^{\beta L}$, and $K_a^{\gamma L}$ are expressed as follows:

$$K_a^{\gamma} = \frac{k_6}{k_5}\frac{k_1}{k_2}K_a^{\beta} \quad (1)$$

$$K_d^{\gamma} = \frac{k_1}{k_2}\frac{k_4}{k_3}K_d^{\beta} \quad (2)$$

$$K_d^{\gamma H} = \frac{k_5}{k_6}\frac{k_8}{k_7}K_d^{\beta H} \quad (3)$$

$$K_a^{\beta L} = \frac{K_d^{\beta H}}{K_d^{\beta}}K_a^{\beta} \quad (4)$$

$$K_a^{\gamma L} = \frac{k_3}{k_4}\frac{k_8}{k_7}\frac{K_d^{\beta H}}{K_d^{\beta}}K_a^{\beta} \quad (5)$$

(1) *Analysis of pH-Dependent Spectral Change.* The apparent acid dissociation constants are expressed by the following equations:

$$K_a^{E} = \frac{([\overline{E_\beta}] + [\overline{E_\gamma}])[H^+]}{[\overline{E_\beta H^+}] + [\overline{E_\gamma H^+}]} = \frac{1 + k_1/k_2}{1 + k_5/k_6}K_a^{\beta} \quad (6)$$

$$K_a^{EL} = \frac{([\overline{E_\beta L}] + [\overline{E_\gamma L}])[H^+]}{[\overline{E_\beta H^+ L}] + [\overline{E_\gamma H^+ L}]} = \frac{1 + k_3/k_4}{1 + k_7/k_8}\frac{K_d^{\beta H}}{K_d^{\beta}}K_a^{\beta} \quad (7)$$

where K_a^{E} and K_a^{EL} are the apparent acid dissociation constants for the free and the 3-indolepropionate bound enzyme, respectively, and the overlines indicate the equilibrium concentrations. The apparent absorption coefficients for the free and the liganded enzymes as functions of pH are expressed as follows:

$$\epsilon_{app}^{E} = \frac{\epsilon_{EH}[H^+] + \epsilon_E K_a^{E}}{[H^+] + K_a^{E}} \quad (8)$$

$$\epsilon_{app}^{EL} = \frac{\epsilon_{EHL}[H^+] + \epsilon_{EL} K_a^{EL}}{[H^+] + K_a^{EL}} \quad (9)$$

(2) *Kinetics on pH-Jump Experiment.* The apparent rate constant of the interconversion of absorbance at 338 and 422 nm induced by the pH-jump, k_{app}^{H}, is expressed as follows:

$$k_{app}^{H} = \frac{[\overline{E_\beta}]}{[\overline{E_\beta H^+}] + [\overline{E_\beta}]}k_1 + \frac{[\overline{E_\beta H^+}]}{[\overline{E_\beta H^+}] + [\overline{E_\beta}]}k_5 + \frac{[\overline{E_\gamma}]}{[\overline{E_\gamma H^+}] + [\overline{E_\gamma}]}k_2 + \frac{[\overline{E_\gamma H^+}]}{[\overline{E_\gamma H^+}] + [\overline{E_\gamma}]}k_6$$

Using eqs 1 and 6, the above equation can be solved as follows:

$$k_{app}^{H} = \frac{k_1 k_2 (k_5 + k_6)K_a^{E} + k_5 k_6 (k_1 + k_2)[H^+]}{k_2 (k_5 + k_6)K_a^{E} + k_6 (k_1 + k^2)[H^+]} + \frac{k_1 k_2 (k_5 + k_6)K_a^{E} + k_5 k_6 (k_1 + k_2)[H^+]}{k_1 (k_5 + k_6)K_a^{E} + k_5 (k_1 + k_2)[H^+]} \quad (10)$$

The rate constants k_1, k_2, k_5, and k_6 are obtained by fitting eq 10 to the experimental results. K_a^{β} and K_a^{γ} are then calculated using eqs 1 and 6.

(3) *Analysis of Apparent Dissociation Constant for 3-Indolepropionate.* The apparent dissociation constant, K_d^{app} is expressed as follows:

$$K_d^{app} = \frac{([\overline{E_\beta}] + [\overline{E_\gamma}] + [\overline{E_\beta H^+}] + [\overline{E_\gamma H^+}])[\bar{L}]}{[\overline{E_\beta L}] + [\overline{E_\gamma L}] + [\overline{E_\beta H^+ L}] + [\overline{E_\gamma H^+ L}]} = \frac{(1 + k_1/k_2) + (1 + k_5/k_6)([H^+]/K_a^{\beta})}{(1 + k_3/k_4)/K_d^{\beta} + (1 + k_7/k_8)([H^+]/K_a^{\beta})/K_d^{\beta H}} \quad (11)$$

Using eqs 6 and 7, $1/K_d^{\beta H}$ and $[H^+]/K_a^{\beta}$ can be written as follows:

$$\frac{1}{K_d^{\beta H}} = \frac{1 + k_3/k_4}{1 + k_7/k_8}\frac{K_a^{\beta}}{K_a^{EL}}\frac{1}{K_d^{\beta}} \quad (12)$$

$$\frac{[H^+]}{K_a^{\beta}} = \frac{1 + k_1/k_2}{1 + k_5/k_6}\frac{[H^+]}{K_a^{E}} \quad (13)$$

Using eqs 12 and 13, eq 11 is solved as follows:

$$K_d^{app} = \frac{1 + k_1/k_2}{1 + k_3/k_4}\frac{1 + [H^+]/K_a^{E}}{1 + [H^+]/K_a^{EL}}K_d^{\beta}$$

or

$$K_d^{app} = \frac{1 + k_5/k_6}{1 + k_7/k_8}\frac{1 + K_a^{E}/[H^+]}{1 + K_a^{EL}/[H^+]}K_d^{\beta H} \quad (14)$$

Fitting of the K_d^{app}−pH plot to eq 14 yields the values of K_a^{E}, K_a^{EL}, $(1 + k_1/k_2)K_d^{\beta}/(1 + k_3/k_4)$, and $(1 + k_5/k_6)K_d^{\beta H}/(1 + k_7/k_8)$. Since k_1, k_2, k_5, k_6 are known from the pH-jump study, the values of $K_d^{\beta}/(1 + k_3/k_4)$ and $K_d^{\beta H}/(1 + k_7/k_8)$ are determined. Defining these values as *A* and *B*, respectively, we obtain

$$K_d^{\beta} = (1 + k_3/k_4)A \quad (15)$$

$$K_d^{\beta H} = (1 + k_7/k_8)B \quad (16)$$

(4) *Kinetics of Substrate Analogue Binding.* The apparent rate constant of the interconversion of absorbance at 338 and

422 nm induced by 3-indolepropionate binding, $k_{app}{}^{L}$ is expressed as follows:

$$k_{app}{}^{L} = \frac{[\overline{E_\beta}]}{[\overline{E_\beta^*}]}k_1 + \frac{[\overline{E_\beta L}]}{[\overline{E_\beta^*}]}k_3 + \frac{[\overline{E_\beta H^+}]}{[\overline{E_\beta^*}]}k_5 + \frac{[\overline{E_\beta H^+ L}]}{[\overline{E_\beta^*}]}k_7 + \frac{[\overline{E_\gamma}]}{[\overline{E_\gamma^*}]}k_2 + \frac{[\overline{E_\gamma L}]}{[\overline{E_\gamma^*}]}k_4 + \frac{[\overline{E_\gamma H^+}]}{[\overline{E_\gamma^*}]}k_6 + \frac{[\overline{E_\gamma H^+ L}]}{[\overline{E_\gamma^*}]}k_8 \quad (17)$$

$$[\overline{E_\beta^*}] = [\overline{E_\beta}] + [\overline{E_\beta L}] + [\overline{E_\beta H^+}] + [\overline{E_\beta H^+ L}]$$

$$[\overline{E_\gamma^*}] = [\overline{E_\gamma}] + [\overline{E_\gamma L}] + [\overline{E_\gamma H^+}] + [\overline{E_\gamma H^+ L}]$$

which is solved using eqs 15 and 16 to be:

$$k_{app}{}^{L} = \frac{k_1 + ([H^+]/K_a{}^{\beta})k_5 + [k_3/(A(1 + k_3/k_4)) + k_7([H^+]/K_a{}^{\beta})/(B(1 + k_7/k_8))][L]}{1 + ([H^+]/K_a{}^{\beta}) + [1/(A(1 + k_3/k_4)) + ([H^+]/K_a{}^{\beta})/(B(1 + k_7/k_8))][L]} + \frac{k_2 + ([H^+]/K_a{}^{\gamma})k_6 + [(k_2/k_1)k_4/(A(1 + k_4/k_3)) + ((k_6/k_5)k_8([H^+]/K_a{}^{\gamma}))/(B(1 + k_8/k_7))][L]}{1 + ([H^+]/K_a{}^{\gamma}) + [(k_2/k_1)/(A(1 + k_4/k_3)) + ((k_6/k_5)([H^+]/K_a{}^{\gamma}))/(B(1 + k_8/k_7))][L]} \quad (18)$$

The kinetic parameters k_3, k_4, k_7, and k_8 are obtained by fitting eq 18 to the experimental points (Figure 7). $K_d{}^{\beta}$ and $K_d{}^{\beta H}$ are obtained from eq 15 and eq 16, respectively, and $K_d{}^{\gamma}$, $K_d{}^{\gamma H}$, $K_a{}^{\beta L}$, and $K_a{}^{\gamma L}$ are from eqs 2−5.

ACKNOWLEDGMENT

We thank T. Yano for helpful discussions.

REFERENCES

1. Newton, W. A., and Snell, E. E. (1964) *Proc. Natl. Acad. Sci. U.S.A. 51*, 382−389.
2. Newton, W. A., Morino, Y., and Snell, E. E. (1965) *J. Biol. Chem. 240*, 1211−1218.
3. Morino, Y., and Snell, E. E. (1967) *J. Biol. Chem. 242*, 2800−2809.
4. Kagamiyama, H., Morino, Y., and Snell, E. E. (1970) *J. Biol. Chem. 245*, 2819−2824.
5. Tani, S., Tsujimoto, N., Kawata, Y., and Tokushige, M. (1990) *Biotechnol. Appl. Biochem. 12*, 28−33.
6. Dementieva, I. S., Zakomirdina, L. N., Sinitzina, N. I., Antson, A. A., Wilson, K. S., Isupov, M. N., Lebedev, A. A., and Harutyunyan, E. H. (1994) *J. Mol. Biol. 235*, 783−786.
7. Kawata, Y., Tani, S., Sato, M., Katsube, Y., and Tokushige, M. (1991) *FEBS Lett. 284*, 270−272.
8. Snell, E. E. (1975) *Adv. Enzymol. Relat. Areas. Mol. Biol. 42*, 287−333.
9. Phillips, R. S. (1989) *J. Am. Chem. Soc. 111*, 727−730.
10. Torchinsky, Y. M., and Kawata, Y. (1994) in *Molecular Aspects of Enzyme catalysis* (Fukui, T. and Soda, K., eds.) pp 186−188, Kodansha, Tokyo.
11. June, D. S., Suelter, C. H., and Dye, J. L. (1981) *Biochemistry 20*, 2714−2719.
12. Kiick, D. M., and Phillips, R. S. (1988) *Biochemistry 27*, 7339−7344.
13. Phillips, R. S., and Gollnick, P. D. (1989) *J. Biol. Chem. 264*, 10627−10632.
14. Phillips, R. S., Bender, S. L., Brzovic, P., and Dunn, M. F. (1990) *Biochemistry 29*, 8608−8614.
15. Phillips, R. S. (1991) *Biochemistry 30*, 5927−5934.
16. Watanabe, T., and Snell, E. E. (1977) *J. Biochem. Tokyo 82*, 733−745.
17. Metzler, C. M., Viswanath, R., and Metzler, D. E. (1991) *J. Biol. Chem. 266*, 9374−9381.
18. Suelter, C. H., and Snell, E. E. (1979) *Methods Enzymol. 62*, 561−568.
19. Suelter, C. H., Wang, J., and Snell, E. E. (1976) *FEBS Lett. 66*, 230−232.
20. Laemmli, U. K. (1970) *Nature 227*, 680−685.
21. Nihira, T., Yasuda, T., Kakizono, T., Taguchi, H., Ichikawa, M., Toraya, T., and Fukui, S. (1985) *Eur. J. Biochem. 149*, 129−133.
22. Isom, H. C., and DeMoss, R. D. (1975) *Biochemistry 14*, 4291−4297.
23. Hayashi, H., Mizuguchi, H., and Kagamiyama, H. (1993) *Biochemistry 32*, 812−818.
24. Ro, H-S., Hong, S-P., Seo, H-J., Yoshimura, T., Esaki, N., Soda, K., Kim, H-S., and Sung, M-H. (1996) *FEBS Lett. 398*, 141−145.
25. Ben, K. T., Markel, A., Gdalevsky, G., Torchinsky, Y. M., Phillips, R. S., and Parola, A. H. (1996) *Biochim. Biophys. Acta 1294*, 147−152.
26. Kallen, R. G., Korpela, T., Martell, A. E., Matsushima, Y., Metzler, C. M., Metzler, D. E., Morozov, Y. V., Ralston, I. M., Savin, F. A., Torchinsky, Y. M., and Ueno, H. (1985) in *Transaminases* (Christen, P., and Metzler, D. E., Eds.) pp 37−108, John Wiley & Sons, New York.
27. Shaltiel, S., and Cortiijo, M. (1970) *Biochem. Biophys. Res. Commun. 41*, 594−600.
28. Johnson, G. F., Tu, J.-I., Shonka Bartlett, M. L., and Graves, D. J. (1970) *J. Biol. Chem. 245*, 5560−5568.
29. Misono, H., and Soda, K. (1977) *J. Biochem. (Tokyo) 82*, 535−543.
30. O'Leary, M. H. (1971) *Biochim. Biophys. Acta 242*, 484−492.
31. Vazquez, M. A., Munoz, F., Donoso, J., and Garcia Blanco, F. (1991) *Biochem. J. 279*, 759−767.
32. Yano, T., Kuramitsu, S., Tanase, S., Morino, Y., and Kagamiyama, H. (1992) *Biochemistry 31*, 5878−5887.
33. Yano, T., Hinoue, Y., Chen, V. J., Metzler, D. E., Miyahara, I., Hirotsu, K., and Kagamiyama, H. (1993) *J. Mol. Biol. 234*, 1218−1229.
34. Sundrarraju, B., Antson, A. A., Phillips, R. S., Demidkina, T. V., Barbolina, M. V., Gollnick, P., Dogson, G. G., and Wilson, K. S. (1997) *Biochemistry 36*, 6502−6510.
35. Woehl, E. U., and Dunn, M. F. (1995) *Coordination Chem. Rev. 144*, 147−197.

BI971995+